Journal of Chromatography B 1162 (2021) 122434

Contents lists available at ScienceDirect

Journal of Chromatography B

journal homepage: www.elsevier.com/locate/jchromb

n-Layer BET adsorption isotherm modeling for multimeric Protein A ligand and its lifetime determination

Ketki Behere, Seongkyu Yoon *

Department of Chemical Engineering, University of Massachusetts Lowell, 1 University Ave, Lowell, MA 01854, USA

ARTICLE INFO

Keywords:
Protein A
Adsorption isotherm
Continuous bioprocessing
Caustic effect
Recombinant Protein A ligand

ABSTRACT

Langmuir and other single-layer adsorption isotherms show the binding behavior of natural Protein A ligands immobilized on a column. However, no models have been shown in literature to explain the adsorption phenomena on the recombinant high binding capacity Protein A resins. This study has characterized the Protein A binding domain distribution across the ligand with multi-layer adsorption isotherms for a recombinant Protein A resin. The adsorption data was analyzed using the Langmuir, Freundlich, Brunauer–Emmett–Teller (BET) and various other mathematical equations. The best fit of experimental data was obtained with n-layer BET model wherein the isotherms of Protein A exhibited Type IV behavior according to BET classification. Furthermore, the binding capacity was studied throughout the shelf life using the multi-layer adsorption isotherm model. Antibody adsorption isotherms of Protein A resin were obtained at preset duration of caustic incubation. The experiments were carried out for two conditions of sanitization agent, namely, caustic and caustic with salt. Static and dynamic isotherm analysis showed that a new resin had a lower binding capacity and the initial sanitization improved the binding capacity, probably by making the binding domains more accessible. The binding capacity at equilibrium, dynamic breakthrough and batch were also evaluated and reported in this paper. The study modeled the multimeric Protein A ligand and established the requirement of optimization for cleaning regime. This study provides a fundamental understanding of the binding patterns in the recombinant Protein A ligands through a working mathematical equation and improves the current knowledge of Protein A resin lifetimes.

1. Introduction

1.1. Protein A ligand

Protein A (ProA) chromatography is an affinity chromatography with a ProA ligand attached to the base matrix through a linker. ProA resins are highly specific to the Fc region of Immunoglobulins (IgG) and hence used in the purification of antibodies [1]. ProA is a membrane protein naturally found in the cell wall of Staphylococcus aureus bacteria [2,3]. ProA binds to the Fc region of the antibody through hydrophobic bonding, ionic interactions and hydrogen bonds. There is a complex interaction with IgG1, IgG2 and IgG4 which leads to a strong bond between ProA ligand and the IgG, while a single substitution of arginine to histidine in the Fc region prevents the IgG3 to bind to Protein A [4–7]. Recombinant ProA (rProA) ligands are engineered with higher specificity to the monoclonal antibody binding (mAb) [8]. ProA ligand is known for its degradation due to caustic, which is traditionally used as a cleaning agent in the bioprocessing [9]. Limited knowledge is available for the fundamental mechanism of degradation [10]. Newer versions of rProA is engineered to be caustic resistant wherein the B domain of natural Protein A is replaced by Z domain [11–13].

1.2. Experimental methods for column integrity test

The current column integrity tests are not cumulative and have minimum relevance in continuous loading scenario. Height Equivalent to Theoretical Plate (HETP) and Asymmetry tests depend on a Gaussian curve to calculate the width of the peak at 50% of peak height. The peak tailing and leading provide valuable information about the column packing [14]. This test is useful for analytical and certain batch preparative purposes where the peak symmetry helps in evaluating the column packing and thereby the column performance. However, the shape of the elution peak is nonlinear and requires complex modifications to the HETP calculations on the changes of the peak shape over time for an overloaded column [15–17]. For a continuous chromatography setup, it is imperative to know how to compensate for the loading

* Corresponding author.
E-mail address: Seongkyu_yoon@uml.edu (S. Yoon).

https://doi.org/10.1016/j.jchromb.2020.122434
Received 18 April 2020; Received in revised form 25 October 2020; Accepted 28 October 2020
Available online 18 November 2020
1570-0232/

volume to the resin degradation. As the column is assumed to be running continuously, any offline methods to check for the column integrity do not prove feasible.

Moreover, there is limited information available for the Protein A ligand performance once it is bound to the base matrix. Resin manufacturers provide the necessary data on the binding capacity, pore size, particle radius, leaching rate, sanitization buffer concentration, number of column cycles, etc. The end user then performs a fixed amount of lab scale studies at a stringent operating conditions for a limited shelf life [18]. Once the specifications are established, the operating conditions are maintained below set standards in manufacturing. There is limited scope for exploring and stretching the boundaries of Protein A lifecycle.

1.3. Adsorption isotherm

Breakthrough curve has been traditionally used to evaluate the column capacity by measuring the protein uptake rate in the bulk and particle phase. Isotherm is the thermodynamic foundation of the chromatography process [19,20]. The change in adsorption isotherm provides a precise way of gauging the column integrity in regards to the binding capacity of the resin. The adsorption isotherm parameters provide the resin characteristics [21]. In a continuous chromatography setup, it is imperative to understand the resin characteristics whilst product quality and purity are not the sole representatives of the how the resin is performing.

Antibody binding to the binding site on the Protein A ligand is via chemical adsorption. There is strong binding (hydrophobic bonding, ionic interactions and hydrogen bonds) which is greater than 35 KJ/mol [22,23]. There is specific surface symmetry required for the chemisorption process. Langmuir isotherm has been reported in literature [24,25] to explain the Protein A resin performance over the specific cycles for a few caustic resistant resins. Langmuir isotherm is an equilibrium model which assumes single layer coverage [26]. The adsorbate is bound to the adsorbent binding site assuming all the binding sites are equally probable. However, the next generation resins are engineered to bind to more than one antibody Fc region as discussed below and hence different isotherms are required to explain the binding mechanisms [27]. The objective of this study is to provide a fundamental understanding of the binding patterns in the recombinant Protein A ligands and improve the current knowledge of Protein A resin lifetimes.

2. BET model framework

2.1. Protein A affinity isotherm

Brunauer–Emmett–Teller (BET) developed a model isotherm known as BET adsorption isotherm which explains the multilayer adsorption [28]. Protein A resin is available as mesoporous particles (5–100 nm) and the BET model can effectively explain adsorption in the given range. The model was developed for adsorption of gases and has been shown to extend to complicated systems.

2.2. Isotherm parameters calculation

All the empirical equations used for the isotherm parameters calculation assumed adsorption with monolayer coverage. The monolayer coverage excludes Freundlich isotherm as it has infinite saturation capacity [29,30].

All the equations used during the model fitting as summarized in the Table 1.

Table 1
Model equations used for curve fitting to isotherm data.

Model	Reference	Mathematical equation
Langmuir	[26,43]	$Q_e = \frac{Q_a^0 K_b C_e}{1 + K_b C_e}$
Freundlich	[29,30]	$Q_e = K^f C_e^{1/n}$
BET	[41,42]	$Q_e = \frac{Q_a^0 K_b x}{(1-x)(1+(K_b-1)x)}$
Modified BET	[34,35]	$Q_e = \frac{Q_a^0 K_b x}{(1-x)(1-K_b \ln(1-x))}$
BET for n-layers	[38,40]	$Q_e = (\frac{Q_a^0 K_b x}{(1-x)}) \frac{(1-(n+1)x^n + nx^{n+1})}{(1+(K_b-1)x - K_b x^{n+1})}$
GAB	[36,37]	$Q_e = \frac{Q_a^0 K_b x K}{(1-Kx)(1-Kx+K_b Kx))}$
Halsey	[38]	$Q_e = (-d/lnx)^{1/e}$
Oswin	[39]	$Q_e = A[x/(1-x)]^B$

x represents Ce/Cs where Ce (mg/mL) is the concentration in the liquid phase and Cs (mg/mL) is the saturation concentration. The curve fitting was performed in MATLAB© R2017a using the Curve fitting toolbox. When Ce << Cs and Kb >> 1 and Kad = Kb/Cs, the BET approaches Langmuir isotherm.

3. Materials

3.1. Feed

Protein A Purified Polyclonal Human Gamma Globulin (HGG) (Product code HS-470-80) from SeraCare Life Sciences (Milford, MA) with a feed concentration of 19.1 g/L was utilized as a feed for the duration of this study. The Immunoglobulin G (IgG) had an approximate molecular weight of 160 KDa, with an extinction co-efficient of 13.8 g/100 mL at 280 nm. The feed was solubilized in Phosphate buffer saline (PBS pH 7.3) and stored at 8 °C until actual usage.

3.1.1. Resin characteristics

Toyopearl AF-rProtein A HC-650F (Tosoh Bioscience, King of Prussia, PA) was used for the equilibrium isotherm study. The resin has a mean pore size of 100 nm and a bead diameter of 30–60 μm [27]. The high capacity resin is obtained from a recombinant strain of Escherichia coli. The base matrix for the resin is polymethacrylate and is covalently attached to the Protein A ligand through a multi-point attachment linker. The high capacity resin can hoist upto six Y-type antibody binding domains within a single Protein A ligand. The Y-type binding domain is engineered from C-domain, which is present in the natural Protein A ligand. The increased number of binding domains in a ligand boosts the ratio of Protein A binding domains to antibodies thereby leading to higher probability to antibody binding on the ligand.

3.2. Isotherm study

3.2.1. 96-deep well plate study

A 96-well plate was used to perform the isotherm experiment for the Protein A lifecycle study. The interior 40 out of 96 wells were used, while excluding the exterior wells of the plate to avoid the edge effect and evaporation loss on the plate. The exterior wells were dispensed with 500 μL of deionized water to account for possible evaporation during the long incubation periods. All the experiments were performed at room temperature. 100 μL of resin slurry was pipetted into each well. The plate was weighed before and after incubation to check for possible leaks. Duplicate runs were performed wherein each concentration was carried out in two different wells. In addition, the new resin data was obtained from four samples for each concentration and each sample was measured in duplicates (total 8 measurements for the new resin concentration). Each absorbance measurement was performed in duplicates.

3.2.2. Resin volume calculation

100 μL of resin slurry was pipetted in six pre-weighed centrifuge tubes while the resin bottle was being constantly stirred. The mass of the dispensed material was measured. The slurry was centrifuged at 3000g for 5 min and the settled volume of dispensed resin was measured with the calibrations of the centrifuge tubes.

3.2.3. Resin characterization

40–50% (v/v) slurry of resin was dispensed. 100uL of the resin slurry was pipetted in each well of the 96-deepwell plate while the resin bottle was being constantly stirred. The resin was then equilibrated, loaded with feed, eluted and sanitized as described below.

3.2.4. Equilibration

The resin was equilibrated with 500 μL of PBS buffer (pH 7.4) in each well. After dispensing, the deep-well plate was covered and kept on the shaker to equilibrate at 150 rpm for 30 min. The deep-well plate was then centrifuged at 3000*g* for 10 min. The supernatant was pipetted out later. These steps were performed four times for complete exchange of storage buffer (for new resin) or caustic (for recycled resin) to equilibration buffer [31]. In the case of new resin (0 hr), the resin was allowed to equilibrate in the PBS buffer overnight on the orbital shaker at 150 rpm.

3.2.5. Protein loading

A stock solution of 19.1 g/L feed and PBS buffer (pH 7.4) was used to prepare the required load concentration. The desired volume of PBS buffer was first added to each well. The required feed was then pipetted in each well with the pipette tip immersed in the liquid to ensure that all the feedstock solution was mixed into the PBS buffer in the well. The pipette tips were replaced after each dispense. The total volume dispensed in each well was 500 μL. Once loaded, the 96-deepwell were covered with a plate tape and parafilm to prevent evaporation. The plate was then placed on an orbital shaker at 150 rpm for overnight incubation. After incubation, the plate was centrifuged at 3000*g* for 5 min. 100 μL of the supernatant was sampled into 96-well plate for absorbance measurement. The plates were then read at 300 nm and 320 nm. Protein calibration curve was generated by standard dilutions of known antibody concentration performed in duplicates.

3.2.6. Elution

0.1 M glycine pH 3.0 was used as a stripping buffer to remove the bound antibodies from the ligands. 500 μL of elution buffer was dispensed in each well and incubated under orbital shaker at 150 rpm for 30 min. After incubation, the 96-deepwell plate was centrifuged at 3000*g* for 5 min. The centrifuged liquid was then decanted. The elution step was performed twice to ensure the complete desorption of the antibodies from the ligands.

3.2.7. Sanitization

After elution, sanitization was performed with 0.5 M caustic. 500 μL of sanitization buffer was dispensed in each well and incubated under orbital shaker at 150 rpm for 30 min. After incubation, the 96-deepwell plate was centrifuged at 3000*g* for 5 min. The centrifuged liquid was then decanted. 500 μL of sanitization buffer was again pipetted in each well and the 96-deepwell plate was then incubated on an orbital shaker for 7.5 h. Post-incubation the plate was centrifuged at 3000*g* for 5 min and the supernatant was removed. Equilibration step was performed as explained in the section above.

3.2.8. Sanitization with salt and caustic

A separate isotherm study was performed to study the effect of addition of salt with caustic during sanitization (0.5 M NaOH + 0.5 M NaCl). The sanitization solution with 0.5 M caustic and 0.5 M NaCl was prepared in deionized water. The equilibration, loading and elution were performed as explained in the sections above. During sanitization, 500 μL of the prepared sanitization solution was dispensed in each well and the 96-deepwell plate was incubated on orbital shaker at 150 rpm for 30 min. After incubation, the plate was centrifuged at 3000*g* for 5 min. The centrifuged liquid was then removed. 500 μL of the prepared sanitization solution was again pipetted in each well and the 96-deepwell plate was then incubated on an orbital shaker for 7.5 h. After the incubation, the plate was centrifuged at 3000*g* for 5 min and the supernatant was removed. Equilibration step was performed as explained in the Equilibration section.

3.2.9. Resin cycling study

The new resin in each of the wells was equilibrated, loaded, eluted and sanitized as summarized above. For a sanitization cycle in a typical chromatography column run, the resin was contacted with caustic for a period of 15 min. During a column chromatography run, caustic was allowed to first equilibrate and then left in static condition to ensure that the resin was cleaned. The 15 min exposure to caustic accounted for one cleaning cycle. The equilibrium concentration for new resin was coined as 0 hr measurement. Thereafter, the resin was contacted with the sanitization agent for 7.5 h during the sanitization step of the new resin. After incubation of the sanitization agent, the isotherm experiment was repeated followed by another 7.5 h of sanitization agent incubation which resulted in 15 h total incubation. Each incubation time of 7.5 h with caustic culminated to 30 cycles of sanitization.

3.2.10. Equilibrium isotherm measurement

The adsorption isotherm explains the equilibrium between the adsorbate (antibody) in the solid phase i.e. bound to the Protein A ligand within the pores and liquid phase (buffer). Different concentrations of antibody were contacted with fixed volume of resin slurry and the antibody concentration was measured in the liquid phase. The adsorbed antibody was calculated by the following equation.

$$Q_e = \frac{(C_0 - C_e)}{Q_{max}} \quad (1)$$

The initial concentration loaded is given by C_0 (mg/mL) and the concentration in the liquid phase is given by Ce (mg/mL) while the maximum binding capacity of Protein A is given by Q_{max} (mg/mL). The number of binding sites of the Protein A ligand occupied by the antibodies is given by Q_e (mg of adsorbed antibody per mg of Protein A ligand).

3.2.11. Dynamic isotherm study

The dynamic isotherm study was performed in a 96-deepwell plate at a concentration of 19.1 g/L in duplicates. 100 μL of the resin slurry was dispensed in each well while the resin bottle was being constantly stirred. The resin was then equilibrated with PBS as explained in the Equilibration section. After loading the feed, the plate was incubated on a shaker for 30 min at 150 rpm. Thereafter, every 30 min, the plate was removed from the shaker and allowed to settle for 5 min. After settling, 50 μL of the supernatant was sampled in a 96 well plate for absorbance measurement. The resin was then eluted and sanitized (caustic with and without salt) as described in the respective sections.

3.2.12. Column chromatography study

3.2.12.1. Breakthrough study. 1 mL columns with Toyopearl rPA HC-650F (company location) were used for the column chromatography study. A feed concentration of 19.1 g/L was used as load. The column was loaded with the purified feed until complete saturation. The saturation was monitored for the effluent with a UV detector. The resin lifetime study was performed with 0.5 M caustic as the sanitization buffer and contact time set to 15 min for one sanitization cycle with the volumetric flow rate maintained at 1 mL/min during the column operations. The column was initially bypassed during load to measure the saturation signal of the UV sensor for feed concentration of 19.1 g/L. The loading with column in line was continued until the load flow through signal was equal to the saturation signal in bypass mode. The breakthrough curve was generated. The column was run at 0 hr for new resin and after every 15 h of incubation with 0.5 M caustic until 60 h.

3.2.12.2. Batch study. The new column with Toyopearl rPA HC-650F

was loaded with the purified feed at 19.1 g/L for 30 CVs or until 22% breakthrough. Similar operating conditions were used as described in the breakthrough study. The column was run at 0 hr for new resin and after every 15 h of incubation with 0.5 M caustic until 60 h.

4. Results & discussion

A range of concentrations was used from a stock of 19.1 g/L purified polyIgG feed to perform the isotherm experiment. The resin was contacted with sanitization buffer for 7.5 h and chromatography steps were repeated to obtain the isotherm curves at various time points. The standard error between the measurements was between 0 and 3%. The human gamma globulin powder contains the same distribution of IgG antibody subclasses as is found in the general human population. IgG subclasses from human IgG which have been previously isolated with an approximate ratio of 66% IgG1, 23% IgG2, 7% IgG3 and 4% IgG4 [5,32]. An enhanced rProtein A ligand is bound to the Toyopearl HW-65F base bead via a multipoint attachment. Weinberg et al showed that while it can be seen that there is competitive binding dynamics in polyIgG wherein desorption of the lower binding IgGs occur to the stronger binding IgGs, the competition occurs over longer time scales (~4 h) and is observed with pH gradient elution study [33]. The IgG species of low elution pH (IgG1), or higher binding strength displace species of higher elution pH (IgG2), or weaker binding strength during pH gradient experiments [33]. The current study was performed in a step elution manner with a low pH (~3.0 pH units) for the batch and breakthrough experiments and with a fixed elution pH for the isotherm experiments. Since the elution pH was consistent throughout the study and the elution

Table 2
Estimated parameters for several models.

	Time of caustic contact	New	7.5 h	15 h	22.5 h	30 h	37.5 h	45 h
Model/Parameters	Cycle #	1	30	60	90	120	150	180
Langmuir	Q_m	29.2	57.7	49.4	44.8	39.7	36.7	80.1
	K_d	−166400	−248000	−1.64E + 05	−1.64E + 05	−1.74E + 05	−1.64E + 05	0.09
	SSE	560	2905	2261	1839	1611	969.8	94.01
	R^2	0.57	0.5	0.49	0.49	0.46	0.55	0.94
	RMSE	9.67	22	19.41	17.51	16.39	12.71	3.96
Freundlich	K_d	6.41	13.8	9.61	8.19	5.2	7.9	6.41
	n	0.7	0.79	0.85	0.85	0.98	0.73	0.7
	SSE	81.45	313.8	300.5	248.6	175.7	105.6	81.45
	R^2	0.94	0.95	0.93	0.93	0.94	0.95	0.94
	RMSE	3.69	7.23	7.08	6.44	5.41	4.2	3.69
BET	Q_{a0}	7.0	17.0	14.0	12.4	10.8	9.4	8.1
	K_b	1.65E + 06	3.29E + 06	2.70E + 06	1.48E + 06	1.39E + 06	8.24E + 05	8.19E + 05
	SSE	644.1	924.4	652.6	620	481.9	801.5	922.4
	R^2	0.51	0.84	0.85	0.83	0.84	0.63	0.4
	RMSE	10.36	12.41	10.43	10.17	8.96	11.56	12.4
BET modified	Q_{a0}	14.8	33.0	27.4	24.4	21.9	19.2	16.9
	K_b	7.71E + 06	46.5	61.5	117	38.8	2.97E + 06	4.73E + 06
	SSE	69.37	30.25	9.98	20.25	10.56	71.3	134.7
	R^2	0.95	0.995	0.998	0.995	0.997	0.967	0.913
	RMSE	3.4	2.25	1.29	1.84	1.33	3.45	4.74
n-layer BET	Q_{a0}	12.8	24.3	19.5	17.8	15.1	16.0	16.1
	K_b	8.91E + 04	1.639 + 05	1.639 + 05	1.639 + 05	1.638 + 06	1.639 + 05	9.47E + 04
	n	6	6	6	6	6	6	5
	SSE	39.47	94.1	112.7	111	32.12	58.75	47.55
	R^2	0.97	0.984	0.974	0.969	0.989	0.973	0.969
	RMSE							
GAB	Q_{a0}	15.2	27.7	22.5	–	17.5	18.8	18.8
	K_b	1.638 + 05	1.638 + 05	1.78E + 05	–	1.638 + 05	1.638 + 05	1.638 + 05
	K	0.75	0.82	0.84	–	0.85	0.77	0.7
	SSE	7.1	32.09	33.11	34.4	2.54	20.39	13.94
	R^2	0.995	0.995	0.993	0.99	0.999	0.991	0.991
	RMSE	1.19	2.53	2.57	2.62	0.71	2.02	1.67
Halsey	d	5189	–	1665	1581	784.8	–	26,320
	e	2.783	–	2.114	2.158	2.045	–	3.131
	SSE	4.78	–	26.94	31.85	4.29	–	6.36
	R^2	0.996	–	0.994	0.991	0.999	–	0.996
	RMSE	0.89	–	2.12	2.3	0.85	–	1.03
Oswin	A	25.22	49.52	40.95	37.06	31.84	31.61	29.72
	B	0.28	0.35	0.37	0.36	0.39	0.3	0.25
	SSE	14.78	49.96	66.95	63.41	20.05	24.32	12.01
	R^2	0.989	0.991	0.985	0.982	0.993	0.989	0.992
	RMSE	1.57	2.89	3.34	3.25	1.83	2.01	1.42

was carried out for a short period (30 min), the effect of the competitive binding on the binding isotherm exist but are considered to be relatively consistent and minimal. As such, most of the binding occurred with IgG1 with the given elution conditions.

4.1. Resin isotherm characteristics

The experimental data was fitted to various mathematical models given in Table 1. The fitted parameters are summarized in Table 2. Several models were used to evaluate the best model that could explain the isotherm characteristics. The isotherm curve showed multi-layer isotherm like-behavior and hence several multi-layer models were used to evaluate the best fit. BET was used for model fitting wherein the maximum binding capacity to form the first layer (Q_{a0}) was high for all sanitization cycles which is expected as the Protein A ligand binds strongly to the antibody due to its ligand affinity nature. Hence a few modifications of BET model were investigated. Modified BET [34,35] isotherm parameters showed higher goodness of fit. The maximum binding capacity however was not congruent with the expectation. GAB [36,37] model fit the data with the highest R^2 for the entire incubation range. However, this multi-layer model showed no difference in K_b contrary to the expectation. Other models like Halsey [38] and Oswin [39] were attempted but were incongruent with the current state of knowledge for chemisorption and high binding at low concentrations. N-layer BET [38,40] model showed a reasonable fit wherein the n represents the number of layers which are formed on the ligand surface. Langmuir and Freundlich are commonly used isotherm models to explain the single layer saturation phenomena, and hence were evaluated. The Sum of Squared Errors of prediction (SSE) was high for all the parameters in the Langmuir model and hence the model was not reliable to explain the empirical data. The R^2 was low for all the parameters in the Langmuir model, except at 45 h (180 cycles), where the R^2 is 0.94 and the SSE is 94.01, suggesting that the resin approaches single layer binding kinetics after considerable exposure to 0.5 M caustic. Freundlich model showed a reasonably good fit for a few timepoints but had limited physical significance. The N-layer model was selected for its significance to the current ligand distribution at hand.

BET with n-layers provided the most logical explanation. When the binding sites for adsorption are limited, the adsorption layer is constrained by n. The n-layer BET expression is reduced to a Langmuir equation when n is unity. As n approaches infinity, the equation results in a classic BET equation. This can be mathematically represented as:

$$\lim_{x\to 1}\frac{Q_e}{Q_a^0}=\frac{n(n+1)K_b}{2(nK_b+1)} \tag{2}$$

There are five types of BET isotherms [41]. Type I is the Langmuir isotherm wherein there is monolayer adsorption and limited adsorption as C_e/C_sapproaches unity. Type II isotherm is mainly for non-porous – macro porous and flat surfaces. The multilayer adsorption shows uniform surface energy and infinite adsorption at saturation concentration. It is given by the classical BET expression. Type III and V signify weak adsorption and show low binding at low concentrations. Type IV isotherm is typically used for mesoporous pore size and reaches a saturation at high concentration of adsorbents. The Protein A resin shows strong binding even at low concentrations and has multimeric domains providing more than one binding site on one ligand. In addition, there are limited binding sites on the ligand resulting in saturation at high concentrations. Hence the Type IV isotherm fits the rProA resin best.

4.2. Ligand distribution

Langmuir isotherm assumes that there is only one antibody-binding domain on a single Protein A ligand wherein the binding domains are arranged in a single layer on the pore surface. In other words the ligand is a monomer such that only one antibody can bind to a ligand. This behavior is observed in other resins like Mabselect, etc. [24]. However, the Toyopearl AF-rProtein A HC 650-F used in this study is a high capacity resin, which is engineered to display hexameric Y-type domains [27]. Each Protein A ligand is thus capable of binding upto six different antibodies. The increased number of binding domains in a ligand improves the ratio of Protein A binding domains to antibodies thereby leading to higher probability to antibody binding [27].

Fig. 1 shows the functional domains in naturally occurring Protein A (top) and high capacity rProtein A (bottom). The Domains E, D, A and B are conserved in the rProtein A. The X-type domain is the cell wall attachment region and hence absent in the recombinant version. However, C-type domain is modified to Y-type domain and further multimerized to form a hexameric chain. The hexameric chain is assumed to facilitate a multi-layer arrangement of antibody molecules during adsorption. The natural Protein A ligand (yellow) has a single C-type binding domain (blue) and is attached to the base matrix (dark grey) via a linker (light grey) as shown in Fig. 1. The rProteinA on the other hand is made up of six Y-type binding domains (green) which are displayed on the tetrahedron ligand.

In the case of gases, the adsorbent is first adsorbed on the surface forming a single layer after which additional gaseous molecules form layers on top of the first adsorbed molecule [40,42,43]. BET model assumes that the heat of adsorption is different for the formation of first layer and the other subsequent layers. However, Protein A ligand adsorption is a chemisorption process and hence equal amount of energy is required for every antibody to bind to the ligand. BET isotherm model has several other assumptions given below:

a. The model assumes Langmuir isotherm applied to every layer
b. There is no transmigration between the layers
c. The model assumes equal energy of adsorption for each layer
d. BET is most favorable wherein, even at low concentration, the ligand is capable of binding to high amounts of antibody.
e. Model assumes lateral interaction between adsorbed molecules when the adsorbed molecules are in close proximity to each other manifesting a multi-layer pattern

Although BET model assumes multi-layer adsorption, while the phenomenon is true for gases, the rPA - antibody interaction is based on chemisorption. The antibodies thus could be binding to the rPA domain in a single layer with a close proximity to the other antibodies. As a result, a lateral interaction between the adsorbed antibodies could be present to manifest the BET multi-layer adsorption. With recombinant technology, there is a possibility of enabling more than one binding domain to the Protein A ligand. As a result, for the same ligand surface area, more than one antibody is able to bind to the ligand.

There is no evidence of interaction in literature between two antibody molecules at the binding site in the natural Protein A ligand. However, the experiments show that it is not true for recombinant Protein A in cases where the antibodies are in close proximity of each other which could lead to lateral interactions between each other. In addition, Monte Carlo simulation studies have demonstrated that entropic effects could also cause a two layer adsorption isotherm for proteins wherein adsorption can lead to chain entropy thereby increasing hydrophobic-polar interactions [44–47]. Koshari et al quantified the nanostructural changes in the resin after the adsorption of a monoclonal antibody (mAbs) under different loading conditions and showed that the large proteins manifest a multi-layer sorption which exhibit volumetric partitioning. Their data suggests that mAbs may accumulate locally in specific regions of the pore space where the mAbs partition from the neighboring resin network due to entropic partitioning. Also, monoclonal antibodies show crowding effects which leads to higher binding capacity and manifest a multi-layer type arrangement. The local crowding could be a mAb-mAb or mAb-resin interactions [47]. Furthermore, Silva et al used the Pearl necklace model to show the

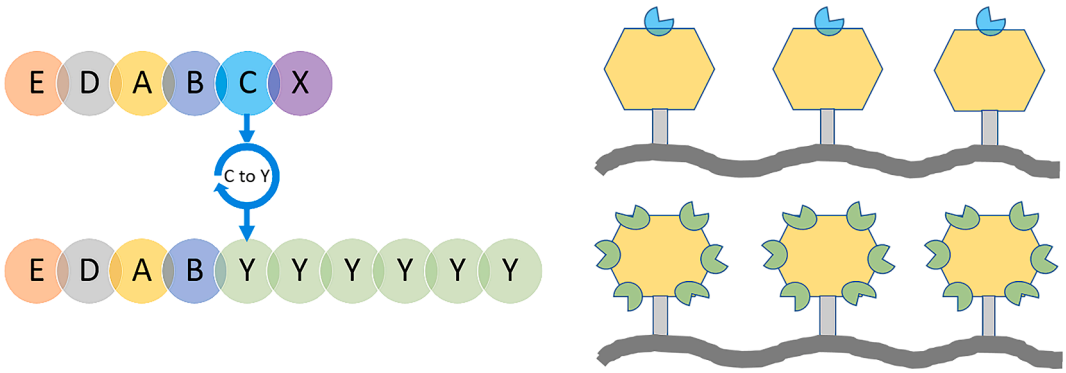

Fig. 1. Schematic of the multi-layer arrangement for the native Protein A (top) and engineered multimeric Protein A (bottom). The natural Protein A ligand (yellow) has A single C-type binding domain (blue) and the recombinant Protein A ligand (yellow) has six Y-type binding domains (green). Both the ligands are shown attached to the base matrix (dark grey) via a linker (light grey). (For interpretation of the references to colour in this figure legend, the reader is referred to the web version of this article.)

molecular mechanisms at the Mabselect SuRe Protein A resin surface. They studied the binding conformations for different ratios of antibody to Protein A stoichiometry via radial density distribution wherein one antibody bound to one Protein A ligand in the linear range of the isotherm while two antibodies were favored to bind to one Protein A ligand in the saturated region [45]. Moreover, the multisite occupancy of adsorbents, which show interactions between each other in this case interactions between antibodies to form aggregates at the Protein A binding site, can be explained by the extension of BET isotherm. In addition, the effects of heterogeneous adsorbent surface could be relevant to the multimeric Protein A ligands and also explained by the extension of BET isotherm. In this context, the multilayer adsorption theory is explained by the n-layer BET isotherm.

4.3. Caustic effect on ligand binding capacity

Fig. 2 shows the adsorption isotherm at various incubation periods of caustic (0, 7.5, 15, 22.5, 30, 37.5 and 45 h). The isotherm for each of the incubation periods from 7.5 h to 45 h shows progressive degeneration of the ligand. However, the isotherm for a new resin at 0 hr shows consistently lower binding capacities as compared to all other runs. Quadruple samples were used to generate the new resin (0 hr) isotherm with duplicate sample measurements. The error between the samples was between 0% and 2%. The isotherm curve for 7.5 h incubation sample (after 30 cycles) showed remarkable increase in binding capacities consistently. Thereafter, the binding capacities and isotherm constant (Kb) reduced gradually. The initial phase of the isotherm curve shows that there is strong binding even at low concentrations of feed. The strong covalent binding is common in affinity binding. There is flattening observed in the mid-phase of the isotherm curve showing that the first layer is saturated on the ligand. This phenomenon is more evident during the longer incubation periods of caustic (37.5 h and 45 h). Thereafter the third phase of the isotherm curve shows sharp increase in binding capacity especially at lower incubation periods (7.5 h and 15 h) showing evidence of multi-layer attachment.

The new resin, which was incubated in equilibration buffer overnight, was later exposed to feed and the isotherm generated, is shown in the Fig. 2. The lower binding capacities for the new resin to form a single layer with Q_{a0} of 12.8 mg/mL could be a result of insufficient bonds being established at the ligand binding site as shown in Table 3. The new resin was exposed to equilibration buffer, feed and elution buffer and sampled for the antibody concentration. The sanitization was performed after the "0 hr" samples. The new resin "0 hr" measurement was

Table 3
Equilibrium adsorption parameters with n-layer BET isotherm.

N-layer BET Cycling time	0.5 M NaOH (mg/mL)	0.5 M Caustic + 0.5 M NaCl (mg/mL)
0 h	12.75	12.75
7.5 h	24.25	25.15
15 h	19.53	17.75
22.5 h	17.8	16.92
30 h	15.07	11.14

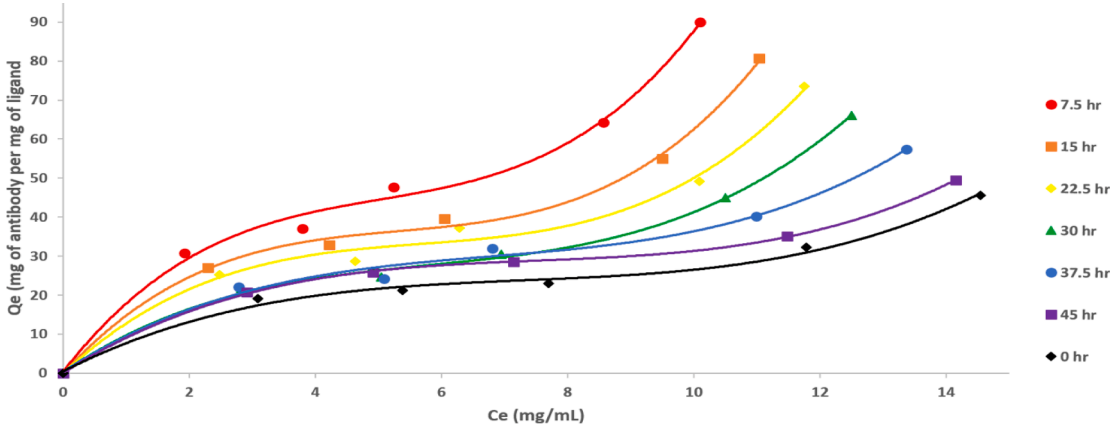

Fig. 2. Isotherm curve to show the effect of caustic on the ligand. The adsorption isotherm at various incubation periods of caustic is plotted for 0 h (black), 7.5 h (red), 15 h (orange), 22.5 h (yellow), 30 h (green), 37.5 h (blue) and 45 h (purple). (For interpretation of the references to colour in this figure legend, the reader is referred to the web version of this article.)

performed after elution without the resin being exposed to sanitization buffer. The new resin study was repeated 4 times (duplicate study for the caustic and caustic + salt buffer condition). In addition each sample was measured in duplicates for accuracy. Post sanitization, the binding capacity of the rProA seem to improve. The salt bridges and hydrogen bonds are hypothesized to be formed at the ligand binding site because of the ionic strength of the sanitization buffer. The salt bridges and hydrogen bonds may not be formed adequately in a new resin due to the tightly bound ligand at the ligand binding site. The high ionic strength of the sanitization buffer appears to open up the covalent bonds near the binding site of the ligand and replaced by the salt bridges, improving the accessibility of the antibody to the ligand binding site. Hence we see a rise in the binding capacity after the first few cycles of sanitization treatment. The phenomenon was evident in the increase of the maximum adsorption capacity to form a single layer Q_{a0} to 24.3 mg/mL which was almost double to the new resin capacity. Thereafter, the isotherm and curve and the corresponding values gradually reduced nevertheless maintained above the 0 hr adsorption curve. The maximum binding capacity to form a single layer was calculated as 24.3 mg/mL which is the binding capacity to form a single layer, and as we observed that there are lateral interactions in addition to the single layer formation, the total maximum binding capacity is higher than 24.3 mg/mL. Between the two loading isotherms at 0hr and 7.5 h, the resin was exposed to elution buffer and sanitization buffer with a contact time of 2 h and 7.5 h respectively. In future studies, it would be worthwhile to investigate the sanitization cycling for the first 7.5 h of incubation. Nevertheless the hypothesis of the caustic effect needs to be confirmed by conformational analysis. Recent studies with Small Angle X-ray Scattering (SAXS) and Small Angle Neutron Scattering (SANS) techniques have shown to be effective to study the protein flexibility and dynamics in a solution [45–50]. Plewka et al demonstrated that more than 1 antibody was bound to the Protein A ligand tetramer by measuring the protein layer thickness and comparing it with the resin radius through SAXS experiments with the Mabselect SuRe recombinant resin [46]. These techniques could be applied to gain improved understanding of the ligand structural modifications during the first few cycles of caustic treatment.

4.4. Influence of salt in caustic wash on ligand binding capacity

The isotherm study was repeated with a sanitization buffer of caustic and salt to evaluate the comparative degradation effects of using salt or no salt in the sanitization buffer. This study showed that there are notable differences between the ligand degradation patterns when a salt is added to the sanitization buffer. However the effect of the salt in the sanitization buffer needs future work to understand the conformational changes within the resin pores. Fig. 3 shows the effect of high concentration salt (0.5 M NaCl) in the caustic wash on the isotherm. A significant improvement in the binding capacity was observed upto 30 h incubation with caustic. Caustic generates ionic interaction with the binding sites of Protein A ligands thereby creating a steric hindrance and reducing the extent of ligand degradation. The high salt concentration showed stronger binding similar to hydrophobic interaction and could be used as a probable mechanism to protect the Protein A ligand from caustic degradation. The isotherm for the incubation periods from 7.5 h to 22.5 h showed increase in binding capacities as compared to the values with only caustic incubation. However, the isotherm for 30 h, 37.5 h and 45 h showed decreased affinities as compared to only caustic incubation values. The data suggests that ionic environment created by salt showed a favorable effect until 22.5 h. Thereafter, the binding capacities fell below the 0 hr binding capacity values. This finding shows that it is imperative to check the effect of excipients for the entire lifecycle of the resin to evaluate the efficiency of the cleaning regime. The hypothesis that the binding capacity of the resin can be improved by the use of salt as an excipient in the sanitization buffer needs to be further confirmed through orthogonal methods namely protein structure analysis. SAXS and SANS techniques could be applied to gain improved understanding of the ligand structural modifications with varying sanitization buffers [45–50]. Furthermore, the equilibrium parameters were estimated using the n-layer BET model for the isotherm experiment with caustic and the experiment with caustic and salt. The maximum binding capacity (mg/mL) to form the first layer (Q_{a0}) is presented in the Table 3. The Q_{a0} for new resin showed lower binding capacity (12.75 mg/mL) as compared to 7.5 h value. The salt showed a mixed effect on the binding capacity wherein until 22.5 h, there was increase or maintenance of ligand stability. Thereafter, the binding capacity to form one layer reduced considerably.

4.5. Dynamic isotherm analysis

The concentration in the liquid phase was measured every 0.5 hr after loading to generate the dynamic curve as shown in Fig. 4. A feed concentration of 19.1 g/L was used for this study. The graph shows the dynamic curve at 0 hr (black), 30 h (red) with only caustic and 30 h with caustic and salt (blue). The residual concentration in the liquid phase confirms the discussion in the above sections. The new resin shows

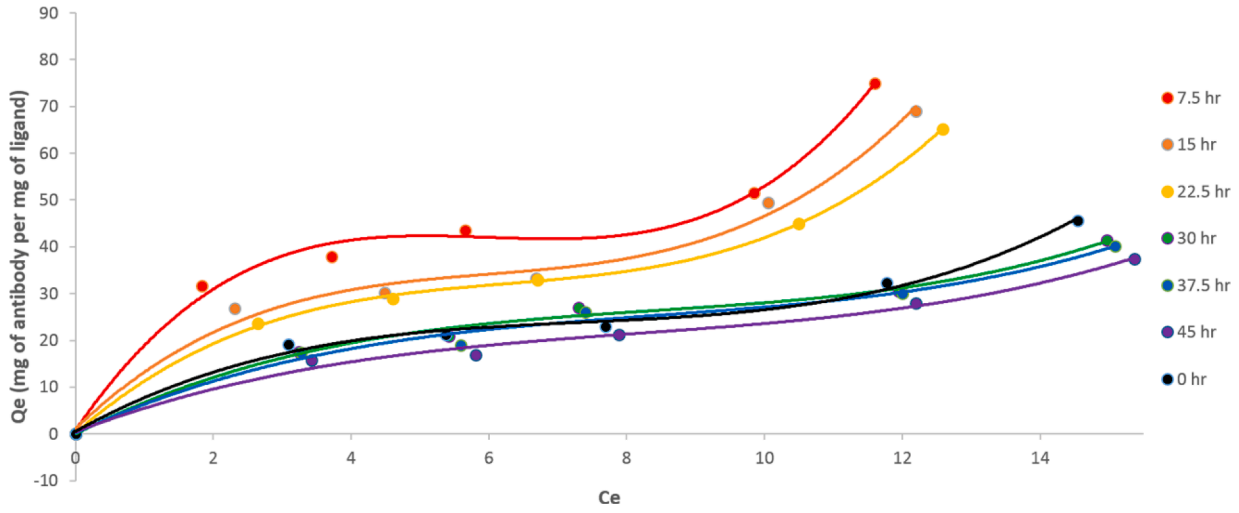

Fig. 3. Isotherm curve to show the effect of caustic and salt on the ligand. The adsorption isotherm at various incubation periods of caustic and salt is plotted for 0 h (black), 7.5 h (red), 15 h (orange), 22.5 h (yellow), 30 h (green), 37.5 h (blue) and 45 h (purple). (For interpretation of the references to colour in this figure legend, the reader is referred to the web version of this article.)

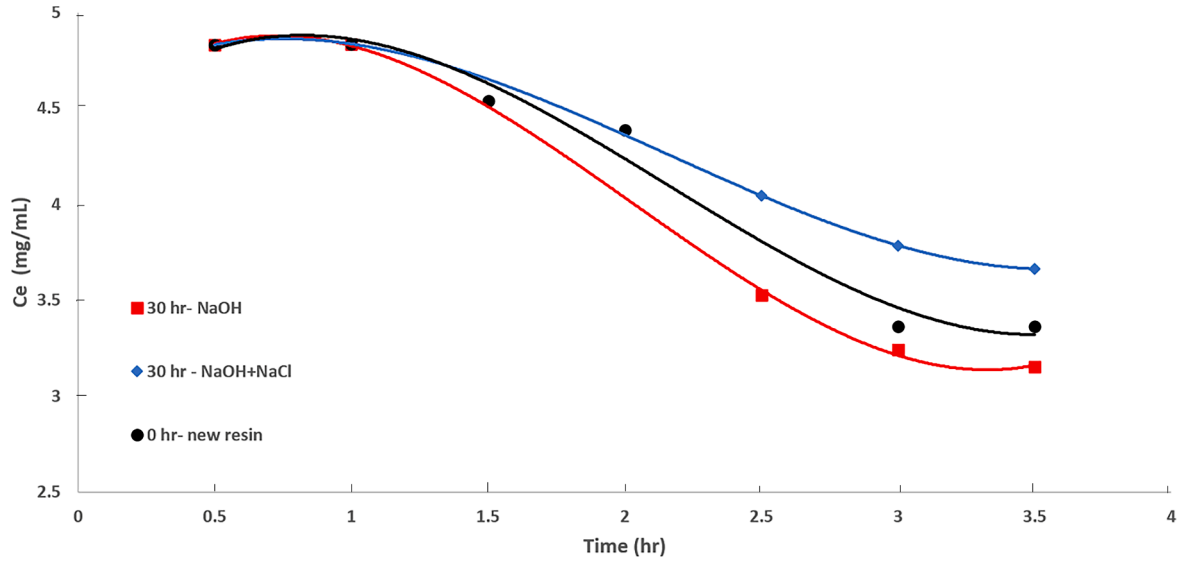

Fig. 4. Dynamic isotherm curve for the residual antibody concentration vs time. The graph shows the dynamic curve at 0 h (black), 30 h with caustic incubation (red) and 30 h with caustic and salt incubation (blue). (For interpretation of the references to colour in this figure legend, the reader is referred to the web version of this article.)

lower binding as compared to 30 h with only caustic incubation but higher loading to 30 h incubation with salt and caustic. The effects are hypothesized to be a result of Donnan equilibrium affecting the micro-environment in the case of caustic with salt and further lead to reduced binding capacity of the ligand binding sites to the antibody.

4.6. Dynamic adsorption in breakthrough loading

The breakthrough curve showed a steep rise for all the runs (0, 15, 30 and 45 h) until 40% breakthrough as shown in Fig. 5. Thereafter, the slope reduced for all the runs and the breakthrough curve creeped slowly to reach complete saturation at around 20 min residence time. The observed shape of the breakthrough curve has been previously observed in literature and is typical for large molecules. The "creeping" phenomenon is observed as a result of the mass transfer resistances from the resin pores to the large antibody molecule. The recombinant Protein A resin used in this study has a mean pore diameter of 100 nm and a mean particle radius of 45 μm. The Human Gamma Globulin G (HGG) has an approximate molecular weight of 160 KDa. For a typical IgG, the viscosity radius is about 7 nm and the molecular diffusion coefficient is very low and is equal about 5×10^{-11} m^2/s [51–53]. Hence, the IgG is excluded from resin pores which are less than about 7 nm. The effective diffusion in the pores is strongly hindered until the pore size becomes larger than ten times the IgG diameter. Based on the above inference, we can conclude that at the beginning of the adsorption process the pores with a diameter of around 70–100 nm are filling fast. Furthermore, the narrower pores take longer to fill proportional to the smaller pore diameter. However, the proposed theory of the observed experimental results needs further understanding of the pore diameter distribution and a comparative experimental study with the simulated breakthrough curves calculated with the General Rate model of the chromatography column. This could be one of the extensions of the current work.

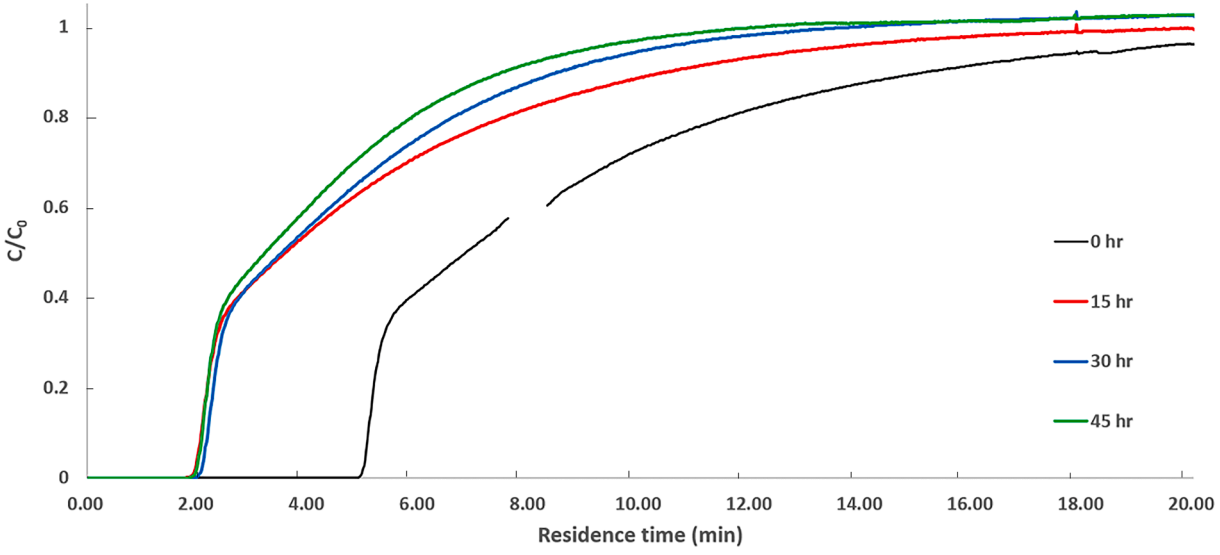

Fig. 5. Breakthrough curve for feed concentration at 19.1 g/L. The graph shows the breakthrough curve at 0 h (black), 15 h (red), 30 h (blue) and 45 h (green). (For interpretation of the references to colour in this figure legend, the reader is referred to the web version of this article.)

4.7. Dynamic adsorption in batch column loading

The batch loading study showed that the column had an early breakthrough for new resin as compared to 15 h incubation with caustic as shown in Fig. 6. This phenomenon suggested that there was improvement in the binding capacity of ligand after exposure to caustic for 15 h. However, no intermediate chromatography runs were performed between 0 hr and 15 h to evaluate and further characterize this finding.

Fig. 6 shows the breakthrough curve for new resin (black), 15 h (red), 30 h (blue), 45 h (green) and 60 h (yellow). A fixed amount of feed (30 CVs) was loaded on the column. The column was washed, eluted and further incubated in caustic for a period of 15 h and the chromatography steps were repeated. While the breakthrough curves at 30 h, 45 h and 60 h showed expected trends, clear distinction in curve was presented for 0 hr and 15 h curve. There was late breakthrough at 15 h, which suggested improved binding capacity as compared to the new resin. The theory that caustic increases the binding capacity of new resin was further validated in the dynamic column study.

4.8. Adsorption isotherm calculation

With the objective of achieving improved understanding of extended loading behavior over lifetime of the resin, higher loading studies were also performed. The experiments, performed to measure adsorption isotherms, were carried out using the same buffers as that of the lifecycle study described above. Feed was loaded at 1.2 g/L and 19.1 g/L onto 1 mL columns of resin B until column saturation. The final equilibrium concentration of residual protein (C_e) was determined at an absorbance of 280 nm which is the industry standard for protein absorbance measurement. The measured absorbance values at 280 nm at 19.1 g/L feed concentration were adjusted for maximum detector limit with a standard graph generated for the UV detector shown in Fig. 2 for different feed concentrations. The absorbance range of the UV detector at 280 nm was calibrated for four concentrations of purified feed viz. 1.2 g/L, 4.8 g/L, 9.5 g/L and 19.1 g/L. The power law was used to calculate the concentration of the load at 70% saturation of the isotherm parameters from these absorbance measurements. The Langmuir isotherm equation was linearized to obtain the isotherm parameters by plotting C_e/q vs. C_e. The protein uptake graph was fitted to the data for 1.2 g/L and 19.1 g/L load concentration to calculate the maximum protein uptake Q_{max} and equilibrium constant K_d from the Langmuir isotherm equation under the described conditions. These adsorption isotherm measurements were recorded for resin B at 0, 15, 30, 45 and 60 h of incubation period for the sanitization buffer (0.5 M caustic), 1 cycle corresponding to 15 min. Hence, the reaction can be dominated by one or combination of the following phenomena

1. Transport of hydroxyl ions within the pores of the resin particle by intra-particle diffusion
2. Interaction of OH^- ions with basic hydrophilic amino acids, such as lysine, arginine, and histidine etc.
3. Interaction of hydroxyl ions with asparagine and glutamine residues on Protein A resin leading to deamidation.
4. Interaction of hydroxyl ions with the polymeric linker chain that links the Protein A ligand to the resin matrix.

The intraparticle and bulk diffusion were assumed to be rapid based on previously reported studies [54,55], and hence the Langmuir isotherm was employed to relate the binding capacity of the resin using the following equation.

$$q = \frac{Q_{max} C_e}{K_d + C_e} \tag{10}$$

Here, Q_{max} represents the total number of binding sites of Protein A that are available to capture IgG, the equilibrium constant, K_d, signifies the affinity of the binding sites to the antibody while q represents the number of binding sites that are currently occupied by the antibodies, loaded at the given concentration C_e. Due to loss of binding sites, there should be a change in the isotherm parameters in particular Q_{max}. In addition, K_d must reduce with increased caustic exposure wherein, the higher the value of K_d, the lower is the affinity of the antibody to the Protein A ligand [56,57].

4.9. Adsorption kinetics

Similar to the breakthrough curves, adsorption isotherm measurements were performed at 0, 15, 30, 45 and 60 h of the incubation period of the resin with 0.5 M caustic of the sanitization buffer. However, these measurements were limited to the resin B only, owing to the fact that it showed the most promising trend with respect to resin performance. The isotherm measurements were recorded at 70% of breakthrough for the resin, and the estimated, Q_{max} and K_d, were recorded and tabulated in Table 4. The Langmuir isotherm was employed to relate the binding capacity of the resin, where q represents the number of binding sites that are currently occupied by the antibodies loaded at the given concentration C_e. The higher values of K_d correspond to lower affinities of the antibody to the Protein A ligand. The maximum protein uptake Q_{max} for

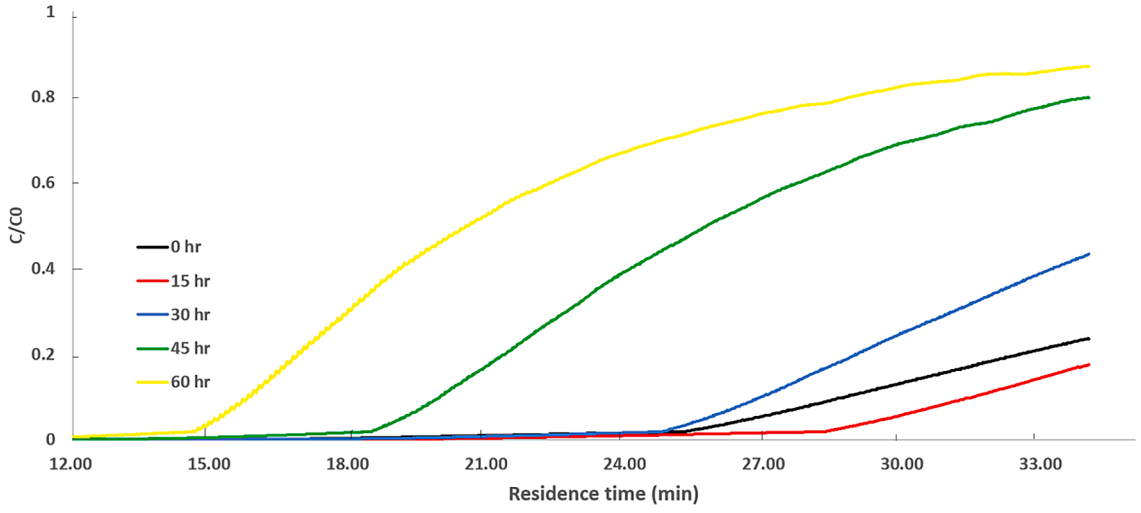

Fig. 6. Batch loading curve at various caustic incubation periods. The graph shows the batch loading curve at 0 h (black), 15 h (red), 30 h (blue), 45 h (green) and 60 h (yellow). (For interpretation of the references to colour in this figure legend, the reader is referred to the web version of this article.)

Table 4
Adsorption parameters with Langmuir isotherm.

Resin B	Q_{max}(g/L)	K_d(g/L)
0 h	87.72	0.000013
After 15 h	42.55	0.00063
After 30 h	38.46	0.00093
After 45 h	37.04	0.0038
After 60 h	31.15	0.0024

resin B decreased from 87.7 g/L to 31.15 g/L at the end of 240 cycles showing 64.5% reduction in the maximum uptake value. The current study recorded the highest equilibrium constant K_d of 0.0024 at the longest loading duration of 60 h, estimating the lowest q value for 60 h as shown in Table 4, while new resin maintained the lowest K_d of 0.000013. This clearly demonstrated the physical and chemical changes transpiring through the lifecycle of the resin, further supporting the proposed degradation kinetics model.

5. Conclusion

This study has characterized the Protein A binding domain distribution across the ligand with multi-layer adsorption isotherms for a recombinant Protein A resin. Antibody adsorption isotherms of Protein A ligand were determined at 0, 7.5, 15, 22.5, 30, 37.5 and 45 h of caustic incubation within the range of 19.1 g/L antibody concentration. The isotherms of Protein A exhibited Type IV behavior according to BET classification. The best fit of experimental data was obtained with n-layer BET model. Further the ligand distribution showed a multi-layer arrangement of the binding domains on the Protein A ligand. Static and dynamic isotherm analysis showed that a new resin had a lower binding capacity and the initial sanitization improved the binding capacity, probably by making the binding domains more accessible. The binding capacity at equilibrium, dynamic breakthrough and batch were also evaluated and reported in this paper. The study modeled the multimeric Protein A ligand and established the requirement of optimization for cleaning regime. This study provides a fundamental understanding of the binding patterns in the recombinant Protein A ligands through a working mathematical equation and improves the current knowledge of Protein A resin lifetimes.

CRediT authorship contribution statement

Ketki Behere: Methodology, Data curation, Formal analysis, Writing - original draft, Writing - review & editing. **Seongkyu Yoon:** Supervision, Funding acquisition, Conceptualization, Methodology, Data curation, Writing - review & editing.

Declaration of Competing Interest

The authors declare that they have no known competing financial interests or personal relationships that could have appeared to influence the work reported in this paper.

Acknowledgments

The study was supported by grants from NSF (1706731) and NSF/IUCRC AMBIC (1624718). The authors gratefully thank Dr. Maurizio Cattaneo for providing the cell-line, and Dr. Kathleen Mihlbachler for providing the lab accessibility and technical guidance and Akshat Gupta for providing objective review and advices during the study.

Appendix A. Supplementary material

Supplementary data to this article can be found online at https://doi.org/10.1016/j.jchromb.2020.122434.

References

[1] S. Ghose, B. Hubbard, S.M. Cramer, Binding capacity differences for antibodies and Fc-fusion proteins on protein A chromatographic materials, Biotechnol. Bioeng. 96 (2007) 768–779.
[2] B. Shopsin, et al., Evaluation of protein A gene polymorphic region DNA sequencing for typing of Staphylococcus aureus strains, J. Clin. Microbiol. 37 (1999) 3556–3563.
[3] M. Graille, et al., Crystal structure of a Staphylococcus aureus protein A domain complexed with the Fab fragment of a human IgM antibody: structural basis for recognition of B-cell receptors and superantigen activity, Proc. Natl. Acad. Sci. 97 (2000) 5399–5404.
[4] R. Lindmark, K. Thorén-Tolling, J. Sjöquist, Binding of immunoglobulins to protein A and immunoglobulin levels in mammalian sera, J. Immunol. Methods 62 (1983) 1–13.
[5] R.C. Duhamel, P.H. Schur, K. Brendel, E. Meezan, pH gradient elution of human IgG1, IgG2 and IgG4 from protein A-sepharose, J. Immunol. Methods 31 (1979) 211–217.
[6] E. Van Loghem, B. Frangione, B. Recht, E.C. Franklin, Staphylococcal protein A and human IgG subclasses and allotypes, Scand. J. Immunol. 15 (1982) 275–278.
[7] B. Recht, B. Frangione, E. Franklin, E. Van Loghem, Structural studies of a human gamma 3 myeloma protein (Goe) that binds staph protein A, J. Immunol. 127 (1981) 917–923.
[8] M. Eliasson, et al., Chimeric IgG-binding receptors engineered from staphylococcal protein A and streptococcal protein G, J. Biol. Chem. 263 (1988) 4323–4327.
[9] K. Behere, B. Cha, S. Yoon, Protein a resin lifetime study: Evaluation of protein a resin performance with a model-based approach in continuous capture, Prep. Biochem. Biotech. 48 (2018) 242–256.
[10] K. Behere, S. Yoon, Chromatography Bioseparation Technologies and In-Silico Modelings for Continuous Production of Biotherapeutics, J. Chromatogr. A 461376 (2020).
[11] S. Gülich, M. Linhult, P.-Å. Nygren, M. Uhlén, S. Hober, Stability towards alkaline conditions can be engineered into a protein ligand, J. Biotechnol. 80 (2000) 169–178.
[12] M. Linhult, et al., Improving the tolerance of a protein a analogue to repeated alkaline exposures using a bypass mutagenesis approach, Proteins Struct. Funct. Bioinf. 55 (2004) 407–416.
[13] S. Hober, K. Nord, M. Linhult, Protein A chromatography for antibody purification, J. Chromatogr. B 848 (2007) 40–47.
[14] J.J. Van Deemter, F. Zuiderweg, A.V. Klinkenberg, Longitudinal diffusion and resistance to mass transfer as causes of nonideality in chromatography, Chem. Eng. Sci. 5 (1956) 271–289.
[15] G. Guiochon, Preparative liquid chromatography, J. Chromatogr. A 965 (2002) 129–161.
[16] A.M. Katti, M. Czok, G. Guiochon, Prediction of single and binary profiles in overloaded elution chromatography using various semi-ideal models, J. Chromatogr. A 556 (1991) 205–218.
[17] S. Ghodbane, G. Guiochon, Optimization of concentration overload in preparative liquid chromatography, J. Chromatogr. A 444 (1988) 275–291.
[18] G. Carta, A. Jungbauer, Protein chromatography: process development and scale-up, John Wiley & Sons, 2010.
[19] Snyder, L.R. Principles of adsorption chromatography; the separation of nonionic organic compounds. (1968).
[20] H.A. Chase, Prediction of the performance of preparative affinity chromatography, J. Chromatogr. A 297 (1984) 179–202.
[21] H. Yang, P.V. Gurgel, R.G. Carbonell, Purification of human immunoglobulin G via Fc-specific small peptide ligand affinity chromatography, J. Chromatogr. A 1216 (2009) 910–918.
[22] C.-C. Lin, Y.-M. Yang, Y.-F. Chen, T.-S. Yang, H.-C. Chang, A new protein A assay based on Raman reporter labeled immunogold nanoparticles, Biosens. Bioelectron. 24 (2008) 178–183.
[23] B. Hammer, L.B. Hansen, J.K. Nørskov, Improved adsorption energetics within density-functional theory using revised Perdew-Burke-Ernzerhof functionals, Phys. Rev. B 59 (1999) 7413.
[24] C. Jiang, J. Liu, M. Rubacha, A.A. Shukla, A mechanistic study of Protein A chromatography resin lifetime, J. Chromatogr. A 1216 (2009) 5849–5855.
[25] R. Hahn, R. Schlegel, A. Jungbauer, Comparison of protein A affinity sorbents, J. Chromatogr. B 790 (2003) 35–51.
[26] R.A. Latour, The langmuir isotherm: A commonly applied but misleading approach for the analysis of protein adsorption behavior, J. Biomed. Mater. Res. Part A 103 (2015) 949–958.
[27] E. Müller, J. Vajda, Routes to improve binding capacities of affinity resins demonstrated for Protein A chromatography, J. Chromatogr. B 1021 (2016) 159–168.
[28] D. Myers, Surfaces, interfaces and colloids, Wiley-Vch New York etc., 1990.
[29] C. Sheindorf, M. Rebhun, M. Sheintuch, A Freundlich-type multicomponent isotherm, J. Colloid Interface Sci. 79 (1981) 136–142.
[30] C. Ng, J.N. Losso, W.E. Marshall, R.M. Rao, Freundlich adsorption isotherms of agricultural by-product-based powdered activated carbons in a geosmin–water system, Bioresour. Technol. 85 (2002) 131–135.
[31] B.K. Nfor, et al., High-throughput isotherm determination and thermodynamic modeling of protein adsorption on mixed mode adsorbents, J. Chromatogr. A 1217 (2010) 6829–6850.
[32] C. Papadea, I.J. Check, Human immunoglobulin G and immunoglobulin G subclasses: biochemical, genetic, and clinical aspects, Crit. Rev. Clin. Lab. Sci. 27 (1989) 27–58.

[33] J. Weinberg, et al., Polyclonal and monoclonal IgG binding on protein A resins—Evidence of competitive binding effects, Biotechnol. Bioeng. 114 (2017) 1803–1812.
[34] F. Jaafar, S. Michaíowski, Modified BET equation for sorption/desorption isotherms, Drying Technol. 8 (1990) 811–827.
[35] P. Schneider, Adsorption isotherms of microporous-mesoporous solids revisited, Appl. Catal. A 129 (1995) 157–165.
[36] E.O. Timmermann, J. Chirife, The physical state of water sorbed at high activities in starch in terms of the GAB sorption equation, J. Food Eng. 13 (1991) 171–179.
[37] Y.H. Roos, Water activity and physical state effects on amorphous food stability, J. Food Process. Preserv. 16 (1993) 433–447.
[38] G. Halsey Jr, A new multilayer isotherm equation with reference to surface area, J. Am. Chem. Soc. 73 (1951) 2693–2696.
[39] C. Oswin, The kinetics of package life. III. The isotherm, J. Chem. Technol. Biotechnol. 65 (1946) 419–421.
[40] R.J. Aguerre, C. Suarez, P.E. Viollaz, New BET type multilayer sorption isotherms. Part II: Modelling water sorption in foods Lebensm. _Wiss. a, Technol. 22 (1989) 192–195.
[41] M. Khalfaoui, S. Knani, M. Hachicha, A.B. Lamine, New theoretical expressions for the five adsorption type isotherms classified by BET based on statistical physics treatment, J. Colloid Interface Sci. 263 (2003) 350–356.
[42] A. Ebadi, J.S. Soltan Mohammadzadeh, A. Khudiev, What is the correct form of BET isotherm for modeling liquid phase adsorption? Adsorption 15 (2009) 65–73.
[43] A. London, An isotherm equation for adsorption on fractal surfaces of heterogeneous porous materials, Langmuir 5 (1989) 1431–1433.
[44] Liu, S.M. (University of British Columbia, 2004).
[45] Molecular mechanisms at the resin interface, L. Silva, G. et al. The pearl necklace model in protein A chromatography, Biotechnol. Bioeng. 116 (2019) 76–86.
[46] J. Plewka, et al., Antibody adsorption in protein-A affinity chromatography–in situ measurement of nanoscale structure by small-angle X-ray scattering, J. Sep. Sci. 41 (2018) 4122–4132.
[47] S.H. Koshari, N.J. Wagner, A.M. Lenhoff, Effects of resin architecture and protein size on nanoscale protein distribution in ion-exchange media, Langmuir 34 (2018) 673–684.
[48] H. Hasegawa, et al., SANS and SAXS studies on molecular conformation of a block polymer in microdomain space, Macromolecules 18 (1985) 67–78.
[49] A.H. Larsen, et al., Combining molecular dynamics simulations with small-angle X-ray and neutron scattering data to study multi-domain proteins in solution, PLoS Comput. Biol. 16 (2020), e1007870.
[50] N. Jouault, et al., Direct measurement of polymer chain conformation in well-controlled model nanocomposites by combining SANS and SAXS, Macromolecules 43 (2010) 9881–9891.
[51] W.M. Saltzman, M.L. Radomsky, K.J. Whaley, R.A. Cone, Antibody diffusion in human cervical mucus, Biophys. J . 66 (1994) 508–515.
[52] M.W. Becker, A.M. Shapiro, Interpreting tracer breakthrough tailing from different forced-gradient tracer experiment configurations in fractured bedrock, Water Resour. Res. 39 (2003).
[53] R. Saber, S. Sarkar, P. Gill, B. Nazari, F. Faridani, High resolution imaging of IgG and IgM molecules by scanning tunneling microscopy in air condition, Scientia Iranica 18 (2011) 1643–1646.
[54] R. Mercadé-Prieto, W.R. Paterson, X.D. Chen, D.I. Wilson, Diffusion of NaOH into a protein gel, Chem. Eng. Sci. 63 (2008) 2763–2772.
[55] T.M. Florence, Degradation of protein disulphide bonds in dilute alkali, Biochem. J 189 (1980) 507–520.
[56] D.D. Do, Adsorption Analysis: Equilibria and Kinetics:(With CD Containing Computer Matlab Programs), vol. 2, World Scientific, 1998.
[57] A. Dada, A. Olalekan, A. Olatunya, O. Dada, Langmuir, Freundlich, Temkin and Dubinin-Radushkevich isotherms studies of equilibrium sorption of Zn2+ unto phosphoric acid modified rice husk, J. Appl. Chem. 3 (2012) 38–45.